AIAA-2003-5242

HIGH TEMPERATURE PERMEABILITY OF CARBON CLOTH PHENOLIC COMPOSITE

O. Y. Park
ATK Thiokol Propulsion,
Science and Engineering Huntsville Operations, Huntsville, AL
T.W. Lawrence
Marshall Space Flight Center/NASA, Huntsville, AL

ABSTRACT

The carbon fiber phenolic resin composite material used for the RSRM nozzle insulator occasionally experiences problems during operation from pocketing or spalling-like erosion and lifting of plies into the char layer. This phenomenon can be better understood if the permeability of the material at elevated temperatures is well defined. This paper describes an experimental approach to determining high temperature permeability of the carbon phenolic material used as the RSRM nozzle liner material. Two different approaches were conducted independently using disk and bar type specimens with the designed permeability apparatus. The principle of the apparatus was to subject a test specimen to a high pressure differential and a heat supply and to monitor both the pressure and temperature variations resulting from gas penetration through the permeable wall between the two chambers. The bar types, especially designed to eliminate sealing difficulties at a high temperature environment, were directly exposed to real time temperature elevation from 22°C to 260°C during the test period. The disk types were pre-heat treated up to 300°C for 8 hours and cooled to room temperature before testing. Nonlinear variation of downstream pressure at a certain temperature range implied moisture release and matrix pyrolysis. Permeability was calculated using a semi-numerical model of quasi-steady state. The test results and the numerical model are discussed in the paper.

INTRODUCTION

Understanding pocketing and ply-lift in solid rocket motor firings is a high priority nozzle task. In the motor firing process with a nozzle lined with a composite insulator, the transport of the gas phase reactant species to and from the interior of the composite insulator is a critical step for understanding these phenomena because they are thought to happen when the internal gas pressure caused by pyrolysis of matrix and volatilization of absorbed gases and moisture builds up within the composite material. Regardless of it being pressure driven or concentration driven, this transport is dependent on the microstructure of the porous media, which is generally expressed in terms of permeability. Fundamental studies of fluid transport through porous media and models for this transport have been reported in various technical areas [1-8] and recently, a model for the transient pressure-driven transport phenomena was proposed [9]

In the experiments, limited numbers of measurements of the gas permeability of composites at room temperature have been reported previously [10,11]. To date, there has been little work devoted to dynamic permeability, as the measurement of permeability at elevated temperature cannot be accomplished by standard measuring techniques [12,13]. Instead of measuring real time permeability, several researches have been conducted at room temperature using pre-charred material, implying that time dependent temperature effect on the permeability due to moisture evaporation and the matrix pyrolysis is eliminated [10, 14]. It was therefore desirable to obtain measurements of the permeability of the material as it is being heated from its virgin states, which was the objective of this effort. This report deals with the dynamic gas permeability of the composite material as a function of temperature.

Measuring a small value of permeability at elevated temperature requires special techniques for which conventional sealing methods are generally impractical or very difficult to implement because of thermal expansion and deformation of seals during the long period of test duration and therefore tends to be unreliable. Among the literature, only Stokes conducted a series of tests with carbon phenolic composite to measure permeability by using a designed apparatus up to 700°C from which he concluded that there are three regimes, pyrolysis and volatized gas diffusion, viscous

matrix flow, and matrix charring events that produce different values of permeability [12]. Significant in this study is that the tests had to be interrupted in the middle of the tests for sealing the specimen.

For our study, a relatively simple test apparatus and specimens were designed: In particular for the real time permeability tests, a bar type specimen of the carbon phenolic was designed to have a permeable wall between two holes that represent upstream and downstream gas chambers and to be heated from the outer surface of the specimens via a heating mantle. For analysis of gas permeability, the well-established Darcy's law has been modified to be a semi-numerical model of quasi-steady state so as to implement temperature dependence to time.

APPARATUS AND SPECIMENS

The permeability equipment incorporated with the specimens was designed and fabricated in-house. Figure 1 shows a schematic drawing of the arrangement of the overall system with the location of instruments and valves, the upstream and downstream chambers and the permeable wall in between. In this design, high pressure was applied to the upstream for a significant pressure differential and regulated to maintain it constant during the test period. Heat was provided through the outer surface of the specimen by means of a heating mantle wrapped around the surface. The heat supply was non-controllable, but its heating rate was reasonably consistent.

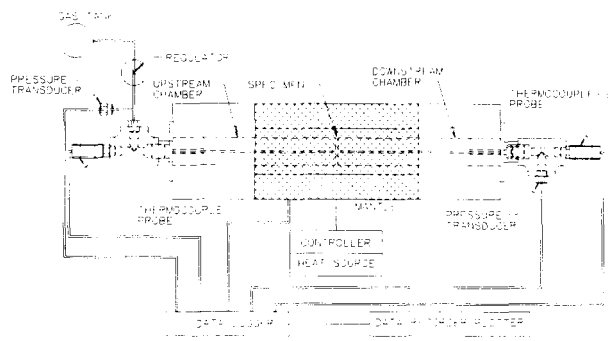

Fig. 1. Schematic Permeability Test Apparatus

The carbon phenolic, denoted as MX4926, was used in the experiments. Two different types of specimens were fabricated as in Fig. 2; one was machined in a disk shape with 1inch diameter and 0.1 inch thickness. This specimen was tested at room temperature after it was heat treated at 300°C in advance. Each specimen was mounted on the ConFlat® flange and cemented using an epoxy based sealing compound. The resulting subassembly was then installed in the test apparatus. The other specimens were fabricated in the shape of bars with two holes in the middle. These are specimens for real time permeability to avoid any leak problems from elevated temperature environment.

The figure shows the physical arrangement of the holes and gas chambers depending on the fluid flow direction versus fiber orientations. For the fill and warp direction tests the holes were coaxially located and for the across-ply direction, the two holes were offset from each other. Note that the offset-hole specimen was fabricated in that way because of a manufacturing limit to the number of fabric layers (maximum thickness of 4.5 inches). The specimen had a large outer wall thickness that at high temperature did not leak under pressure in the presence of surface imperfections. The permeable wall between two chambers had a diameter of 1" and the thickness of 0.1" in consideration of very low permeability.

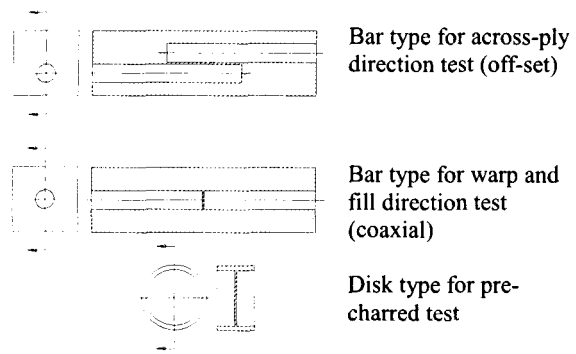

Fig. 2. Permeability Test Specimens

Two pressure responses of the experiment were monitored electrically with piezoelectric transducers designed to operate over a designated pressure range from 0.1-0.45MPa and 0.1-1.8MPa. Two thermocouple probes were also implemented to monitor temperature of the inside chambers. The emf outputs of the transducers and the probes were delivered to an external data acquisition system and then monitored on a PC with a compiled algorithm for automatic recording. Copper gaskets and Swagelok® fittings sealed all the connections. The bar type specimens were assembled and sealed to the apparatus using stainless steel threaded adapters with a high temperature-sealing compound. Note that no mass flow meter was implemented in this design in consideration of very small gas flow rate. The upstream chamber was directly connected to a regulated source of argon/nitrogen and subject to a constant high pressure while the downstream chamber was totally confined. Tee connectors, i.e., three-port connectors, were employed

to accommodate both the transducers and the probes for measuring the chamber environments.

TESTS

Gas permeability was measured on two different types of specimens in a similar way. The only difference was that one used a heat source that provided heat in real time and the other not. At the start of a test, the upstream chamber was immediately pressurized to a designated pressure while downstream chamber was maintained at atmospheric pressure to establish a large pressure differential. The gas flow was initiated through the specimen by slowly establishing a pressure gradient between the two chambers. As the pressure began to rise in the downstream chamber, it was monitored and from this pressure increase, the permeability was calculated. For the real time testing with the bar type specimens, temperature was also monitored and recorded. Fifteen disk type specimens and twelve bar type specimens (four from each direction) were tested. For the real time tests, the specimens were heated up to the instrument limit (260°C).

The local moisture content and matrix pyrolysis rate in the specimen are important parameters in determining the permeability. For these properties, the entire disk type specimens were tested to measure their moisture contents and volatile products in advance. The results in Fig. 3 showed about 0.33-0.39% weight loss at 65°C for 12 hours, 1.57-1.61% loss at 150°C for 12 hours, and 5.70-5.78% loss at 315°C for 5 hours.

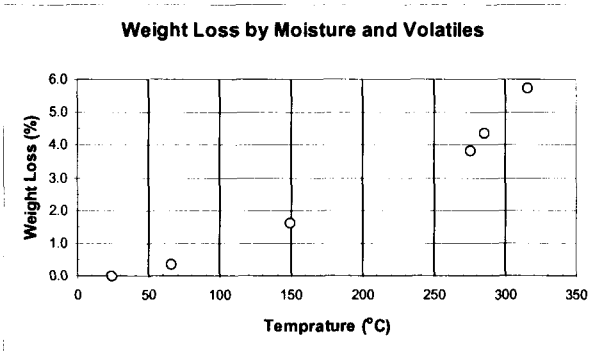

Fig. 3. Weight Loss by Moisture and Volatiles

From this result it was expected that evaporated moisture and volatiles from the inner surface wall of the downstream chamber- about 6" long- would contribute to error in the permeability calculation, but not significantly.

In the room temperature tests with the disk type specimens, only the downstream pressure was recorded periodically while the upstream pressure was kept constant around 0.8-1.8MPa. For the real time permeability tests, the specimens were pressurized at room temperature to find permeability of cold material for about an hour and then they were heated repeatedly. As mentioned earlier, the heating rate was not controllable but it was reproducible. Figures 4-6 show both up and downstream pressure and temperature of the first real time tests. Note that pressure drop from the peak represents a reverse flow as the upstream chamber became emptied. This part of result is additional valuable information for determining the permeability at a lower pressure, but it has been not attempted yet. From the pressure drop curves of the with-ply specimens in Figs. 4 and 5, it is evident that sudden openings in the permeable wall at a certain environmental condition occur. Repeated test results supported this conclusion and the openings became permanent as the material failure when cyclic thermal loads were enforced. Several significant observations are as follows: Since heat was supplied from the outer surface of the specimen there is about 5 minutes time lag for the gas and the chambers to be thermally affected. During this time period, the downstream pressure increases linearly. The upper limit of the instruments terminated the tests by shutting off the gas supply at the downstream pressure of around 0.45MPa.

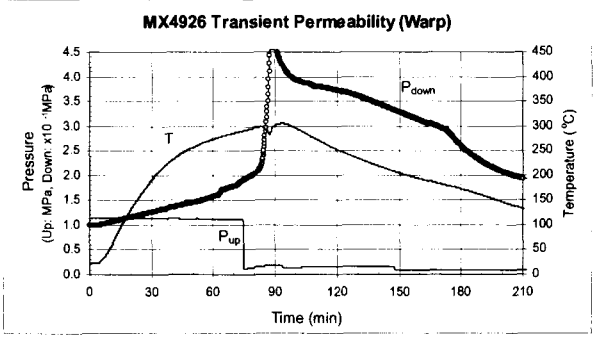

Fig. 4. Real Time Pressure Variation of Warp Direction Specimen

In Figs 4 and 5, the downstream pressure suddenly started to jump up near 290°C. This should be caused by material deformation or cracking/delamination accompanied with the matrix pyrolysis. Also sudden temperature drop from the peak indicates increase in the gas flow rate (Upstream temperature was always superior to the downstream temperature because of the cold transport media). Temperature recovery is followed just after the shut-off as a transient reverse flow is being established. In Fig. 4, irregular pressure profile at the reverse flow situation is due to the shut-off valve operation. Relatively longer periods of heating

in Figs 5 and 6 than in Fig. 4 are related to the specimen size. The across-ply test result in Fig. 6 shows no pressure jump like in the with-ply results, which might be explained in terms of discontinuity of openings at each carbon fabric layer. Cause of deviation of the upstream pressure from the intended value is unknown but it was manually corrected. However this did not cause an error in the evaluation.

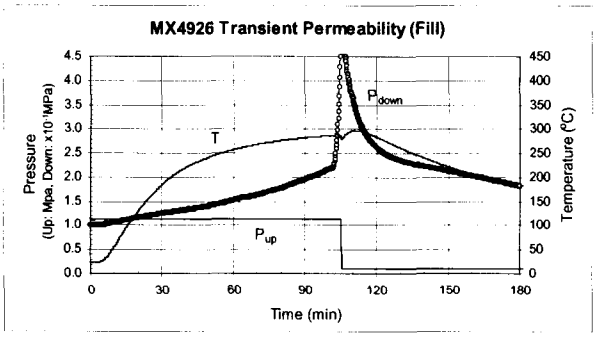

Fig. 5. Real Time Pressure Variation of Fill Direction Specimen

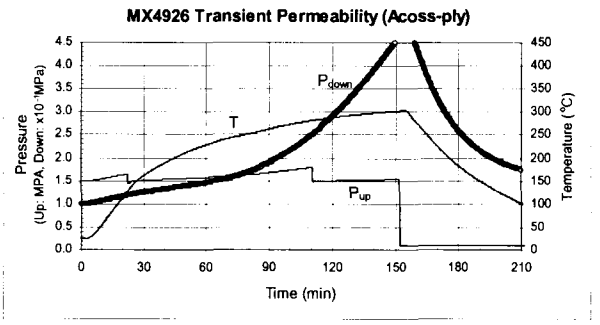

Fig. 6. Real Time Pressure Variation of Across-ply Direction Specimen

PERMEABILITY ANALYSES

In flow studies through porous media, it is customary to present the results in the form of permeability as a function of the mean pressure [15-21]. In general, the inlet volume flow rate and pressure drop across the permeable wall determine the flow condition. However, as mentioned earlier, flow rate was not measured. Instead, rate of change in thermal properties in the system were utilized to evaluate the permeability by means of a modified Darcy's equation [10]. Furthermore in this study, to implement the thermal effect on the permeability the original formula has been expanded to accommodate a temperature gradient. Note that to find an exact value of permeability requires porosity measurement of the material. As can be seen in most literatures [10-12], the cross sectional area in the formula is taken to be equivalent to that of the specimen chamber, which in theory should be the area occupied by the gas paths. Since the porosity of the material varies with temperature, a systematic bias should be involved in the calculation of the flow coefficients. Thus even a detailed quantitative permeability in the literature cannot represent the exact value of permeability. In this study, two modified Darcy's equations were introduced. One has an exact form for isothermal cases and the other has a semi-numerical form to cover thermal effect. The former has an expression of permeability, k, as

$$k = \frac{\mu h V_2}{P_1 A t} \ln\{\frac{(P_1 + P_2)(P_1 - P_{20})}{(P_1 - P_2)(P_1 + P_{20})}\} \text{----------(1)}$$

and the latter has

$$k = \frac{2\mu h V_2}{A T_2 (P_1 - P_2)(\frac{P_1}{T_1} + \frac{P_2}{T_2})} \{\frac{\Delta P_2}{\Delta t} - \alpha \frac{P_2}{T_2} \frac{\Delta T_2}{\Delta t}\} \text{---(2)}$$

where h: permeable wall thickness, $\mu(T)$: gas viscosity, V_2: downstream volume, A: cross-sectional area, t: time, P: pressure, and T: temperature. Subscripts 1 and 2 represent upstream and downstream respectively, and 0 denotes the initial condition. Assumptions in the derivation of Eq. (1) include: one-dimensional mass transfer with constant transport area, constant temperature, and constant physical properties. These assumptions have been stated or implied by numerous workers since the results are likely to be reasonable especially when the ratio of the confining pressure to the initial pressure is high [22]. In Eq. (2), rate of pressure and temperature changes in the downstream chamber governs the permeability. In an isothermal case this expression is identical to the formula in the literature [10]. A correction factor, α ($0 \leq \alpha \leq 1$) is artificially employed in the last term of Eq. (2) for taking care of temperature inhomogeneity in the downstream. Note that the recorded data of inside temperature only represent the highest value in the system. Although most portions of the test apparatus were well covered with an insulation blanket to prevent heat loss from the hood, the loss through the extended pipes and the pressure transducer is inevitable. Through this study a value of 0.4 was chosen.

Figures 7-10 show permeability results from the both equations. Figure 7 represents permeability of the disk type specimens that were pre-heated and then cooled to

room temperature before testing. The result shows the permeability in the same range regardless of the fiber orientation, which implies a higher porosity in the material due to the matrix pyrolysis. The order of permeability is the same as that reported in the literature [14]. This result is valuable for comparison with the results from the real time tests.

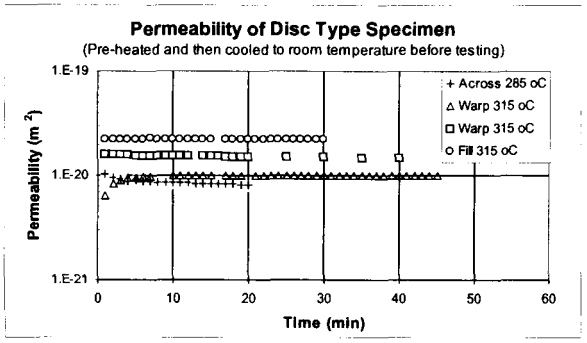

Fig. 7. Permeability of Disk Type Specimen

The bar type specimens were subjected to test at room temperature before they were heated up. Then each specimen was repeatedly heated until a permanent material failure took place. The first tests from three different direction specimens give unique solutions for the permeability in accordance with linear increases in the downstream pressure with time (Marked with the triangles in Figs. 8-10).

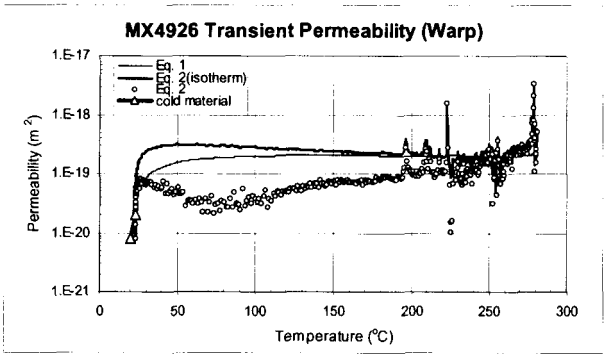

Fig. 8. Real Time Permeability of Warp Direction Specimen

Figures 8-10 express typical results of permeability from the first (pressurized only) and the second (both pressurized and thermally loaded simultaneously) calculated using Eqs. (1) and (2). These figures show how the permeability responds to temperature. It is noticeable that general trends of permeability calculated from Eq. (1) and Eq. (2) with an isothermal condition are closer to each other except at the lower temperature range although their expressions contain different variables. Local fluctuation in the value of permeability from Eq. (2) may be caused by an unsuitable time interval (5-10sec).

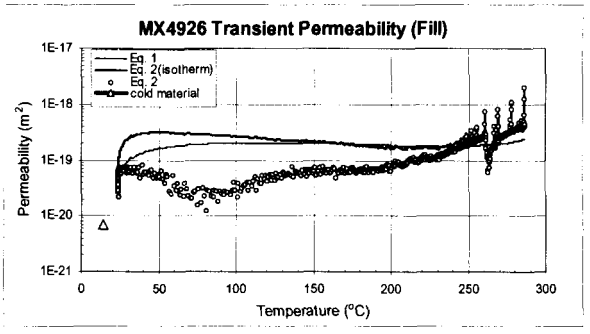

Fig. 9. Real Time Permeability of Fill Direction Specimen

The latter represents in theory the upper limit of the real time permeability for the case of positive temperature gradient. In the isothermal result from Eq. (2), general trend shows decrease in permeability up to the glass transition temperature of the matrix and then continuous increase. Note that rapid increase in permeability occurs during the transient state at the beginning. Though results from warp and fill direction permeability tests are similar in terms of magnitude and fluctuation style, the results from the across-ply tests are not. Finally, Eq. (2) seems to reveal effects from moisture evaporation and glass transition by significantly changing the permeability at 40-65°C and 200-280°C ranges. It is evident that severe fluctuation of permeability occurs during the glass transition period. For the case of the across-ply tests as shown in Fig. 10, the degree of fluctuation is remarkably reduced. Note that the discontinuity at 125°C corresponds to the upstream pressure adjustment.

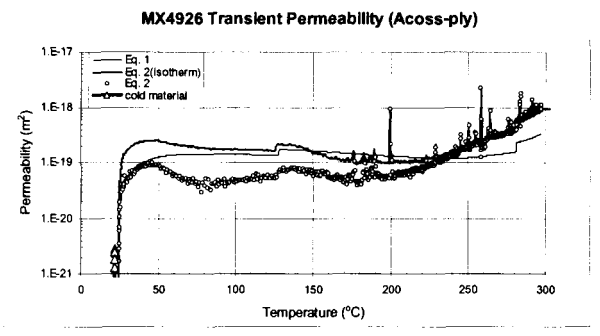

Fig. 10. Real Time Permeability of Across-ply Direction Specimen

Visual examination of the tested specimens revealed that the specimens had cracked or delaminated after repeated thermal loads as shown in Fig. 11-13. Figure

11 is a CT scan of the fill direction specimen that showed relatively higher flow rate in the first real time test. The image is not clear enough to show any cracks or recognizable size gas paths in the permeable wall section, but the density profile in the picture implies less density toward the center of the wall.

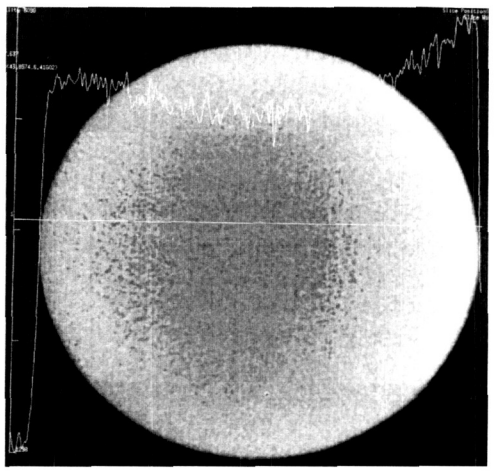

Fig. 11. CT Scan on Post-test Permeable Wall of Fill Direction Specimen (Darker represents lower density in the circular area as seen from the density curve)

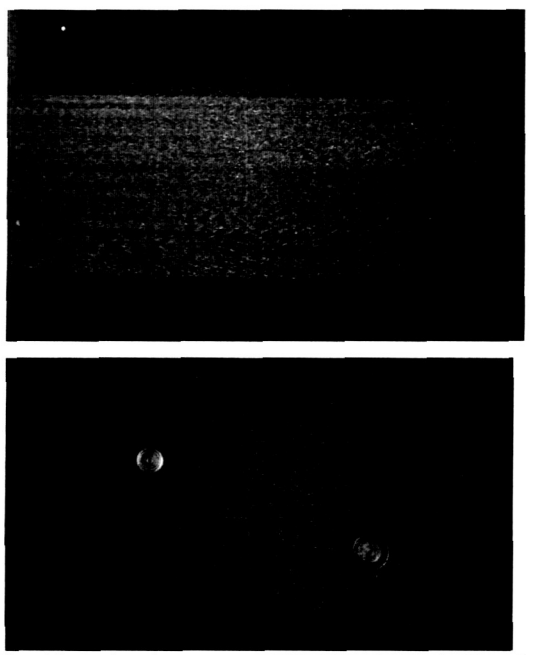

Fig. 12. Delaminated Surface of Across-ply Specimen after Repeated Thermal Loads

Figure 12 shows how the across-ply specimen delaminated by thermal loads with the outer surface temperature of 370-400°C. Note that the delamination highlighted by wetting occurred randomly. The second picture, a dissected section of the specimen in half, shows delamination in the permeable wall. It is uncertain that any effect on the permeability was produced by this kind of delamination.

Figure 13 shows damage on the surface of the warp direction specimen. A soap test seems likely to show a plaid pattern of cracks, but a microscopic examination reveals anisotropic cracks in the matrix with the dominant direction parallel to the fiber orientation. It was reported that the carbon phenolic material could survive in the permeability tests up to 705°C [12]. Material failures at relatively lower temperature in this study might have been caused by cyclic thermal loads for long time periods (3-8 hours per cycle).

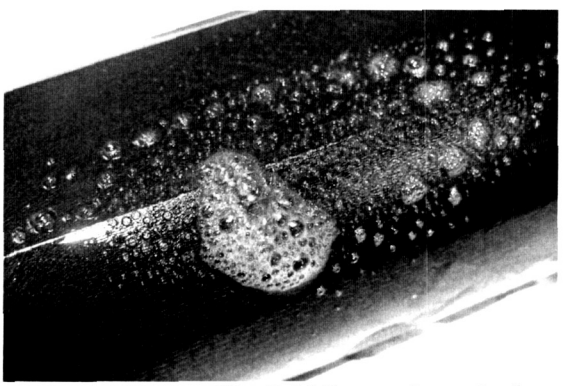

a. A Plaid Pattern like Bubbling on Outer Surface during the Leak Test

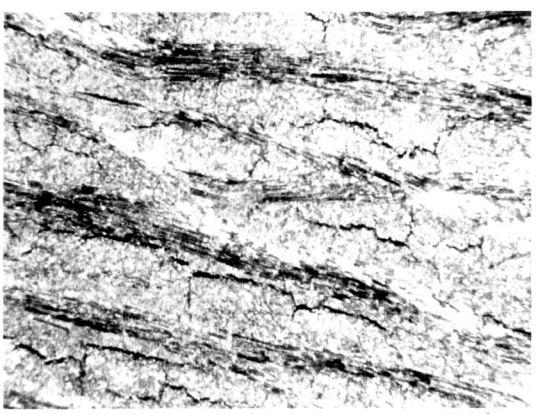

b. Microscopic View of Cracks on Outer Surface (Crack orientations are anisotropic)

Fig. 13. Cracks on Outer Surface of Warp Direction Specimen after Repeated Thermal Loads

CONCLUSION

Two different types of tests were conducted to measure permeability of the carbon cloth phenolic composite at room temperature and at elevated temperature up to 260°C using the designed apparatus and test specimens. This is the first reported attempt at real time permeability testing without any interruption during the test period to understand pocketing and ply-lift phenomenon experienced in the solid rocket motor firings.

A new experimental method for reliable measurement of gas permeability in composite materials has been developed. Key characteristics of this method are the use of bar type specimens and implementation of methods to ensure sealing at the high temperature region with a simple apparatus. Multiple measurements with a limited number of specimens were reproducible and accurate enough to provide information about nonlinear behavior of permeability of carbon phenolic with respect to temperature. The permeability variations in the warp and fill direction specimens are very similar to each other, while they are different from the across-ply direction specimens.

A newly developed semi-numerical formula described thermal effects on the material, especially by moisture evaporation and matrix pyrolysis, properly in the permeability calculations, by revealing local fluctuations near the moisture evaporation temperature and glass transition temperature ranges, respectively. At above the transition temperature range, the permeability increased drastically because of deforming, cracking, or delaminating of material.

As the permeability is nonlinear to temperature, it is presumed that changes in permeability at a very severe environment like a solid rocket motor chamber within a relatively short time period may not be predictable from what was observed in this study. The future work will include extending temperature range, maintaining uniform temperature in the downstream, installing flow meters, improving formula for a higher accuracy, etc. It is expected to present results of permeability from the reverse flow situations and from the repeated thermal loads in the near future.

ACKNOWLEDGEMENTS

The authors are grateful to those who contributed to this program: Matthew Lansing (NASA/MSFC), Anthony Day, Michael Kovach, Michael Cornelius, and Troy Daugette (ATK Thiokol Propulsion).

REFERENCES

1. B.H. Brinkman, "A Calculation of the Viscous Force Exerted by a Flowing Fluid on a Dense Swam of Particles," Applied Scientific Research, Vol. A1, pp. 27-34, 1949.

2. H.C. Brinkman, "On the permeability of Media Consisting of Closely Packed Porous Particles," Applied Scientific Research, Vol. A1, pp. 81-86, 1949.

3. D. Cornell & D.L. Katz, "Flow of gases through Consolidated Porous Media," Industrial and Engineering Chemistry, pp. 2145-2152, 1953.

4. B. Keramati & C.H. Wolgemuth, "The Permeability of Fine-Pored Carbons to a Variety of Gases," Carbon, Vol. 11, pp. 273-280, 1973.

5. R.A. Greenkorn, *Flow Phenomena in Porous Media: Fundamentals and Applications in Petroleum, Water and Food Production*, Marcel Dekker, New York, 1983.

6. M.S. Koefoed, E. Lund, & L. Lilleheden, "Simulation of the VARTM Process for Wind Turbine Blades," 15th Nordic Seminar on Computational Mechanics, Oct. pp. 123-126, 2002.

7. M.O. Saar & M. Manga, "Permeability-porosity Relationship in Vesicular Basalts," Geophysical Research Letters, Vol. 26, No. 1, pp. 111-114, 1999.

8. M.W. Dunn, "Investigating Fluid Flow through Fabrics," National Textile Center Annual Report, M98-P02, Nov. 2000.

9. D.M. Roy, B.E. Scheetz, J. Pommersheim & P.H. Licasttro, "Development of Transient Permeability Theory and Apparatus for Measurements of Cementitious Materials," Strategic Highway Research Program, SHRP-C-627, National Research Council, Washington D.C., 1993.

10. H.L.N. McManus, "High-temperature Thermo-chemical Behavior of Carbon-Phenolic and Carbon-Carbon Composites," Ph.D. Dissertation, Stanford University, pp. 73-86, 1990.

11. T.L. Starr & N. Hablutzel, "Measurement of Gas Transport through Fiber Preforms and Densified Composites for Chemical Vapor Infiltration," J. of American Ceramic Society, Vol. 81. No. 5, pp. 1298-1304, 1998.

12. E.H. Stokes, "Dynamic Permeability of Carbon Phenolic Composite as a Function of Temperature," JANNAF Rocket Nozzle Technology Subcommittee Meeting, MSFC, Huntsville, AL, Oct. 18-20, 1988.

13. E.H. Stokes, "With-Ply Permeability of Carbon Phenolic Composites as a Function of Across-Ply Compressive Load and Temperature," JANNAF Propulsion Meeting, Anaheim, CA, Oct. 3-5, 1990.

14. Southern Research Institute, "Characterization of Six MX4926 Composite Materials with Varying Resin Content and Carbonized Fabric Rinse Water," Final Report, SRI-ENG-97-309-9115.15, Dec.1997.

15. R.R. Bird, W.E. Stewart, & E.N. Lightfoot, *Transport Phenomena,* p. 150, 1960.

16. J. Bear and Y. Bachmat, *Introduction to Modeling of Transport Phenomena in Porous Media*. Kluwer Academic Publishers, Boston, MA, 1990.

17. F.A.L. Dullien, *Porous Media: Fluid Transport and Pore Structure*, 2nd Ed., Academic Press, San Diego, CA, 1992.

18. *Perr's Chemical Engineer's Handbook*, 7th Ed., McGraw-Hill, 1997.

19. D.L. Johnson, J. Koplik, & R. Dashen, "Theory of Dynamic Permeability and Tortuosity in Fluid-Saturated Porous Media," J. of Fluid Mechanics, Vol. 176, pp. 379-402, 1987

20. H.C. Tien & K.S. Chiang, "Non-Darcy Flow and Heat Transfer in a Porous Insulation with Infiltration and Natural Convection," J. of Marine Science and Technology, Vol. 7, No. 2, pp. 125-131, 1999.

21. P.B. Nedanov & S.G. Advani, "A Method to Determine 3D Permeability of Fibrous Reinforcements", J. of Composite Materials, Vol. 36, No. 2, pp. 143-158, 2002.

22. J.D. Wooton & J.D. Wakerly, "Influence of Test Conditions on the Water Permeability of Concrete in a Triaxial Cell," Material Research Society Symposium, MRS Press, Pittsburgh, PA, 1989.